International Journal of Thermophysics, Vol. 15, No. 5, 1994

Measurement and Prediction of Ultrasonic Speed Under High Pressure in Natural Gases

P. Labes,[1] J. L. Daridon,[1,2] B. Lagourette,[1] and H. Saint-Guirons[1]

Received September 16, 1994

Ultrasonic-speed measurements have been performed on two natural gases with significantly different compositions. The systems have been investigated from 12 to 70 MPa in the temperature domain from 263 to 413 K. Furthermore, the ultrasonic-speed data obtained are compared with the values predicted by means of various equations of state.

KEY WORDS: equation of state; high pressure; natural gas; ultrasonic speed.

1. INTRODUCTION

Predictive simulation of the behavior of reservoir fluids during the various stages of their production necessitates the use of fluid state models developed from thermophysical data concerning appropriately selected synthetic mixtures. In this respect, multiphase equilibria, density, and specific heats are properties which, when known over wide ranges of temperature and pressure, provide useful information. However, such measurements are difficult to perform at high pressures, particularly in the case of systems which do not exist in a single-phase state at atmospheric pressure. Speed of sound, which can also be considered as a thermodynamic quantity (and one which can be determined to a high degree of accuracy, including in the high-pressure domain), can contribute valuable supplementary information. This property can be used as a reference property in the development of thermodynamic models, as a supplement to classical properties (volumetric quantities, phase equilibria). It can also be used as a discriminating quantity during comparative tests of different existing models.

[1] Laboratoire Haute Pression, Centre Universitaire de Recherche Scientifique, Université de Pau, Avenue de l'Université, 64000 Pau, France.

[2] To whom correspondence should be addressed.

0195-928X/94/0900-0803$07.00/0

This feature explains why the use of ultrasound as a technique for the acquisition of thermodynamic data has progressed from the exploratory stage to systematic use in a number of laboratories.

The discovery and increasingly widespread production of reservoirs in which fossil fluids are stored at very high temperature and pressure conditions requires experimental procedures adapted to these specific conditions of temperature T and pressure P. The research presented in this paper deals with the ultrasonic speed to two natural gases with fairly significantly differing compositions, up to a pressure of 70 MPa and at temperatures extending over a range of approximately 100 K above normal temperature. These ultrasonic speed data were then compared with the values calculated by various predictive models. The first model tested is the generalized correlation of Lee–Kesler [1], which is a three-parameter corresponding-state application (reduced pressure, reduced temperature, acentric factor). The second model, called AGA 8, is a very accurate equation of state especially set up for gaseous mixtures. Initially developed by Starling [2] to predict the compressibility factor of gases, AGA 8 was later modified by Savidge and Shen [3] to improve its predictive abilities on speed of sound and some other thermophysical properties. Finally the experimental data have been used to test the prediction capacities of some more common equations of state principally used to calculate phase equilibria and density.

2. MEASUREMENTS

To perform ultrasonic speed measurements in fluids subjected to pressures above several hundred bar, pulse techniques have been found to be the most appropriate. Hence, the apparatus used for this study was based on this principle. It has already been described in detail in a previous paper [4]. However, in the cases of fluids with a high degree of attenuation (such as mixtures rich in very light hydrocarbon compounds), only the first echo is sufficiently sharp to be exploited. In this case the classical pulse echo overlap method is inadequate. It is preferable to replace it with a method based on direct chronometry of the travel times taken for acoustic waves to travel through the fluid samples, as described in a paper by Daridon [5]. Thus the error due to the method of determination is lower than 0.06%. There are, however, two further sources of error. The first stems from the uncertainty with respect to temperature (of the order of 0.1 K) resulting essentially from the difficulty in ensuring thermal regulation of the cell. The second source of error is connected to the quality of the pressure probe, which operates to an accuracy of 0.1% over the whole scale.

Table I. Composition of Mixture G1

Component	Mole fraction (%)
Nitrogen	3.187
Methane	88.405
Carbon dioxide	1.490
Ethane	5.166
Propane	1.176
Methyl-2-propane	0.149
N-Butane	0.226
Methyl-2-butane	0.056
N-Pentane	0.049
Isohexanes	0.0216
N-Hexane	0.0136
Benzene	0.0272
Cyclohexane	0.0065
Isoheptanes	0.0100
N-Heptane	0.0041
Methylcyclohexane	0.0052
Toluene	0.0030
Isooctanes	0.0029
N-Octane	0.0008
Isononanes	0.0009
N-Nonane	0.0002

The two multicomponent systems (called G1 and G2), supplied by the company GAZ DE FRANCE, are condensate gases, the respective compositions of which are indicates in Tables I and II. These mixtures were studied at the temperatures at which they are in the single-phase gaseous state, independently of the pressure imposed. The experimental results concerning the ultrasonic speed determinations (associated with signals of frequency 2 MHz) are listed in Tables III and IV, in which speeds are expressed as $m \cdot s^{-1}$.

Table II. Composition of Mixture G2

Component	Mole fraction (%)
Nitrogen	0.496
Methane	89.569
Ethane	8.348
Propane	1.197
Isobutane	0.149
N-Butane	0.226
Isopentane	0.015

Table III. Ultrasonic Speed u ($m \cdot s^{-1}$) in G1 Mixture

	T(K)							
P(MPa)	262.4	273.1	283.8	294.0	303.3	313.6	334.0	354.0
12	393.1	397.2	405.0	413.6	421.4	430.1	446.5	461.7
14	428.0	422.8	424.6	429.3	434.8	441.6	455.8	469.8
16	469.7	455.5	450.7	450.6	452.8	457.2	468.0	480.2
18	511.5	490.6	479.9	475.1	474.3	475.8	482.8	492.4
20	553.0	527.5	511.8	502.6	498.6	497.2	499.7	506.5
22	591.9	563.7	544.0	531.2	524.3	519.9	518.2	521.8
24	628.4	598.3	575.9	560.2	550.5	543.7	537.7	538.4
26	664.3	632.6	607.4	589.4	577.7	568.7	558.6	556.1
28	696.0	663.7	637.2	617.8	604.1	593.0	579.6	574.3
30	727.1	694.4	666.9	645.5	630.4	617.8	600.6	593.1
32	756.8	723.3	694.4	672.3	656.0	641.8	622.9	611.8
34	784.2	750.4	721.3	698.2	680.7	665.5	643.5	630.6
36	810.8	776.6	747.3	724.1	705.3	689.1	665.3	650.3
38	835.8	801.9	772.0	748.9	728.9	711.4	686.0	669.2
40	860.1	826.1	795.9	772.4	751.5	734.1	706.5	687.9
42	883.1	849.3	818.8	794.5	774.2	756.0	726.8	706.9
44	904.8	871.3	840.8	815.7	794.9	776.3	746.4	725.2
46	926.4	893.2	862.7	837.2	816.4	797.3	766.2	743.9
48	947.0	913.6	883.2	857.8	836.4	816.7	785.1	761.4
50	967.2	933.5	903.6	878.1	856.4	836.2	803.5	779.0
52	986.9	953.5	923.2	897.6	876.3	855.3	822.0	796.7
54	1005.3	972.5	942.3	916.2	894.8	873.6	840.0	813.3
56	1023.7	991.0	960.5	934.7	912.7	891.9	857.5	830.5
58	1041.4	1008.7	978.7	952.3	930.9	909.7	874.8	846.9
60	1058.6	1026.3	996.2	969.8	948.0	926.5	891.4	863.0
62	1075.8	1043.4	1013.4	987.0	965.3	944.0	908.0	879.3
64	1091.4	1059.9	1030.0	1004.0	981.8	959.6	923.7	894.5
66	1107.8	1076.4	1046.7	1019.9	998.5	977.0	939.7	910.5
68	1123.3	1091.8	1062.7	1035.9	1014.3	992.3	955.0	925.4
70	1138.7	1107.2	1077.8	1051.8	1029.6	1008.1	970.5	940.1

As an illustration we have plotted, respectively, in Figs. 1 and 2 the isotherm curves and a few isobar curves characterizing the behavior of ultrasonic speed u versus the variables P and T, for the sample G1. Similar sets of curves were plotted for the sample G2 (Figs. 3 and 4). It should be stressed that significant differences appear with respect to the behavior of the ultrasonic speed observed in the liquid state. Whereas for the latter, the isotherm curve sets $u(P)$ or isobar surve sets $u(T)$ are shown to be regular (monotonic and nonintersecting), this is not true for the gaseous mixtures considered. Concerning the speed isobars, one can observe the following.

Table IV. Ultrasonic Speed u ($m \cdot s^{-1}$) in G2 Mixture

	T(K)										
P(MPa)	272.9	293.7	303.4	313.2	323.3	333.2	343.4	353.2	373.4	393.5	413.6
20	549.3	514.7	508.0	505.1	504.6	505.2	507.6	510.8	519.1	528.7	538.5
22	587.6	545.7	535.8	529.9	526.6	525.2	525.8	527.4	533.2	541.0	549.5
24	624.3	577.2	564.5	555.9	550.3	546.6	545.2	545.3	548.6	554.4	561.4
26	659.5	608.7	593.6	582.9	574.9	569.3	566.0	564.5	565.1	568.9	574.4
28	692.3	638.3	621.3	608.9	599.1	591.8	587.0	583.9	581.9	583.8	587.9
30	723.6	667.6	649.4	635.3	623.7	615.1	608.4	604.2	599.5	599.3	601.7
32	753.6	696.4	676.8	661.0	647.9	638.0	629.8	624.2	617.4	615.1	616.2
34	780.9	723.3	702.6	686.0	671.9	660.5	651.3	644.5	635.4	631.5	630.7
36	808.8	749.7	728.3	710.7	695.3	683.2	672.9	665.3	654.0	648.1	646.0
38	834.2	774.7	753.0	734.4	718.2	705.1	693.8	685.3	672.2	664.7	661.1
40	858.6	799.1	776.6	757.8	740.6	726.8	714.7	705.3	690.5	681.4	676.5
42	882.3	822.7	800.2	780.7	762.8	748.2	735.4	725.1	708.7	698.2	692.1
44	905.5	845.2	822.3	802.1	783.8	768.9	755.0	744.4	726.6	714.6	707.3
46	927.2	867.6	844.1	823.9	804.8	789.5	775.0	763.5	744.5	731.3	722.8
48	948.6	888.2	864.9	844.3	825.1	809.0	794.2	782.2	762.0	747.5	738.1
50	969.7	909.0	885.4	864.6	845.0	828.6	813.2	800.7	779.5	763.9	753.4
52	989.4	929.3	905.6	884.5	864.6	847.9	832.1	819.0	796.8	780.4	768.7
54	1008.3	948.5	924.8	903.5	883.5	866.2	850.5	837.0	813.6	796.1	783.6
56	1027.6	967.9	943.6	922.8	902.3	885.0	868.5	854.8	830.2	812.1	798.7
58	1045.7	986.2	962.4	940.6	920.0	902.7	885.9	871.7	846.6	827.7	813.6
60	1063.4	1004.1	980.2	958.7	937.6	919.9	903.0	888.4	862.6	842.9	828.2
62	1080.7	1021.7	997.8	976.1	955.0	937.0	919.9	905.1	878.7	858.6	843.0
64	1097.6	1038.7	1014.7	992.9	971.6	953.5	936.3	921.1	894.5	873.4	857.2
66	1114.0	1055.4	1031.7	1009.9	988.2	970.1	952.4	937.2	909.6	888.4	871.6
68	1130.1	1071.9	1047.7	1025.6	1004.1	986.0	968.5	952.8	925.2	903.0	885.7
70	1146.6	1088.0	1063.7	1041.7	1020.2	1002.0	983.9	968.2	940.5	917.8	899.8

- At the highest pressures, the $u(T)$ curves are monotonic and decreasing, a behavior connected with a value <0 of the temperature coefficient $(\partial u/\partial T)_P$, as for the liquid phase.
- At the lowest pressures the curves go through a minimum, a phenomenon corresponding to a reversal of sign of the same coefficient, which can thus become positive as for the ideal gas.

Similar observations can be deduced from an examination of the ultrasonic speed isotherm curve sets. They exhibit an inflexion on the isotherms relative to the highest temperatures as well as crossover of the various curves in a narrow zone of the plane. At pressures lower than those of the point of intersection (of the order of 20 MPa), the coefficient $(\partial u/\partial T)_P$ is >0, whereas the trend is reversed at higher pressures. These observations

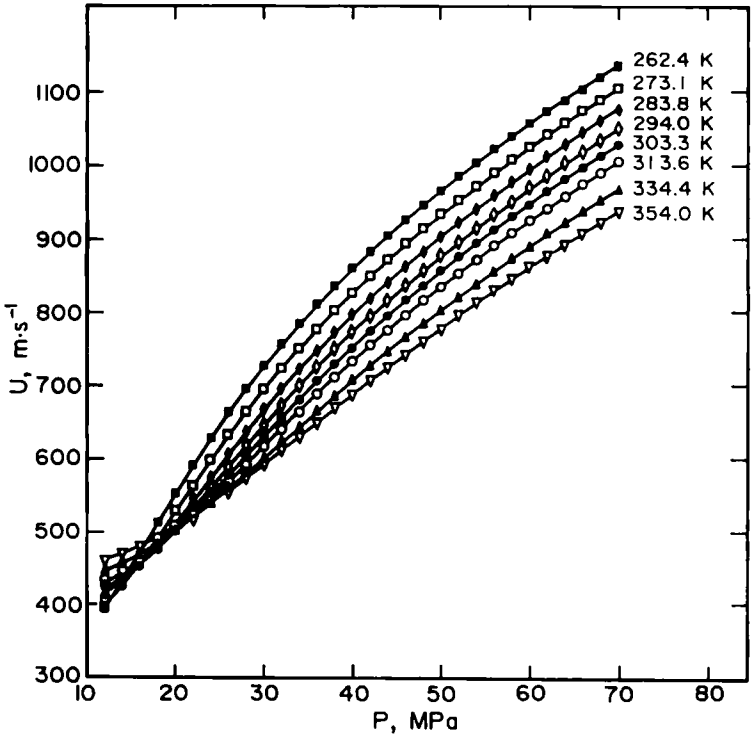

Fig. 1. Variations of ultrasonic speed versus pressure, at constant temperature (measured in sample G1).

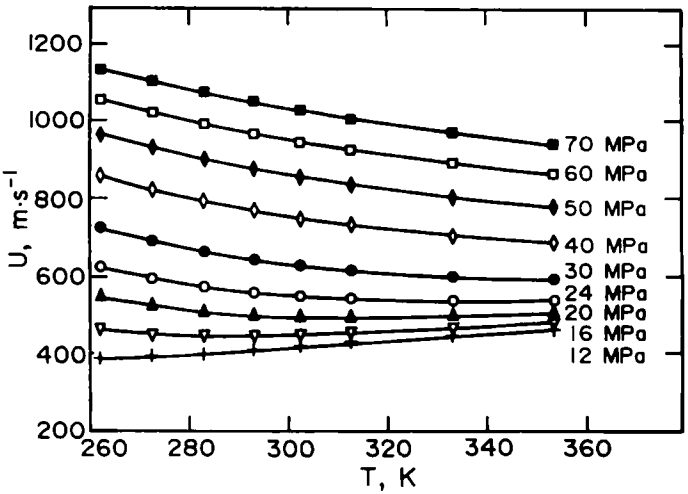

Fig. 2. Variations of ultrasonic speed versus temperature, at constant pressure (measured in sample G1).

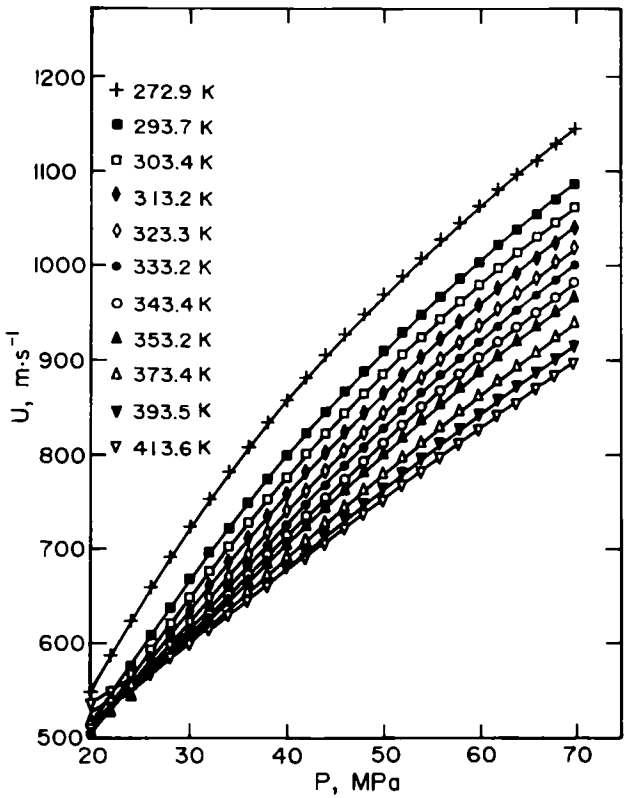

Fig. 3. Variations of ultrasonic speed versus pressure, at constant temperature (measured in sample G2).

are consistent with previous work on pure substances in the gaseous state such as nitrogen, carbon dioxide [6], or gaseous mixtures comparable to those envisaged in this study [7].

The intersections of the speed isotherms make the graph difficult to read. But if the ultrasonic speed is represented versus density and no longer versus pressure, the intersections disappear and the ultrasonic speed appears in these mixtures to be a very regular function, increasing with both density to temperature as shown in Fig. 5.

It should be pointed out in this respect that the density data needed to represent the $U(\rho)$ curves were generated with the aid of AGA8 [2]. This model predicts density with a sufficient accuracy (less than 0.5% in the P, T range investigated) to provide a good plot of the $u(\rho)$ curves.

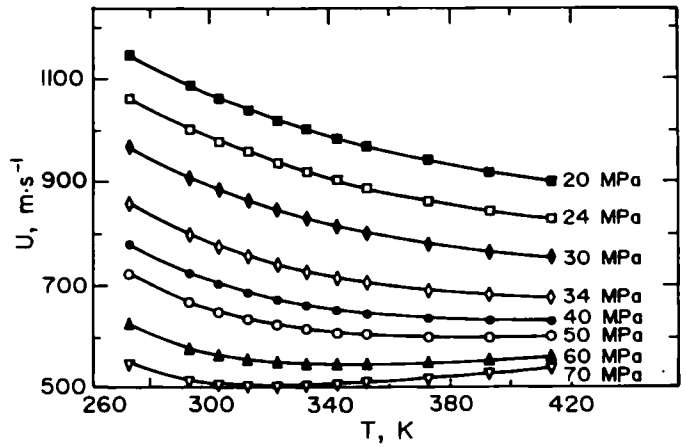

Fig. 4. Variations of ultrasonic speed versus temperature, at constant pressure (measured in sample G2).

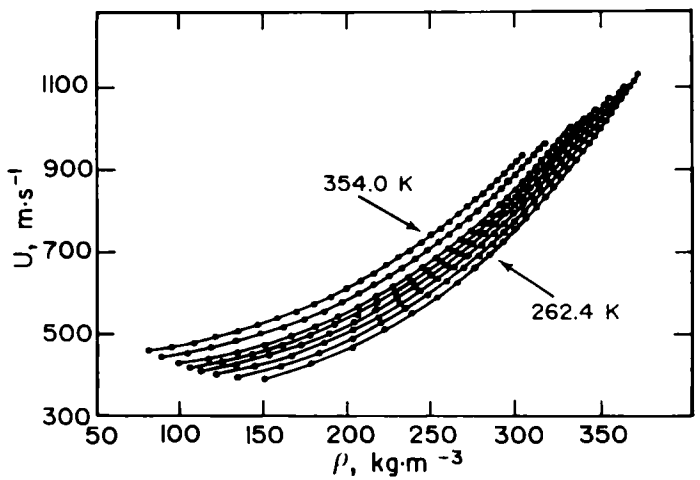

Fig. 5. Isotherm curves characterizing variations of ultrasonic speed, measured in sample G1, versus density.

3. PREDICTION

Combining the relationship linking the ultrasonic speed u to the adiabatic compressibility coefficient β_s,

$$\beta_s = \frac{V}{Mu^2} \tag{1}$$

and the relationship linking the isothermal compressibility coefficient β_T and the adiabatic compressibility coefficient β_s:

$$\beta_T = \beta_s + \frac{VT\alpha^2}{C_p} \tag{2}$$

(in which α designates the thermal expansion coefficient, C_p the molar heat at constant pressure, M the molecular weight, and V the molar volume), one obtains for the speed,

$$u^{-2} = \frac{M}{ZRT}\left[\left\{1 - \frac{P}{Z}\left(\frac{\partial Z}{\partial P}\right)_T\right\} - \frac{RZ}{C_p}\left\{1 + \frac{T}{Z}\left(\frac{\partial Z}{\partial T}\right)_p\right\}^2\right] \tag{3}$$

where $Z = PV/RT$ represents the compressibility factor.

Equation (3), valid for fluids and particularly suitable for gases, shows that a knowledge of ultrasonic speed data in gaseous mixtures can be used as an element of comparison when one wants to check equations of state and in particular their derived forms with respect to temperature and pressure. Following the method described in previous papers [8, 9], a comparative study of the predictive abilities of various models has been performed with reference to the ultrasonic data measured on the gaseous systems. The models selected for these tests are listed below.

3.1. Cubic Equations of State

These equations, commonly used in chemical engineering, are particularly convenient to manipulate for phase-equilibrium calculations. Among them, we selected the most famous.

(i) SRK: Soave–Redlich–Kwong's [10] equation, the general form of which is

$$P = \frac{RT}{V-b} - \frac{a(T)}{V(V+b)} \tag{4}$$

(ii) PR: Peng–Robinson's [11] equation, also of cubic form and involving two parameters, which can be developed as follows:

$$P = \frac{RT}{V-b} - \frac{a(T)}{V(V+b)+b(V-b)} \tag{5}$$

(iii) PR-RP: Peng–Robinson's equation corrected by translation along the volume axis according to a proposal made by Peneloux–Rauzy–Freze [12], the correction effect consisting in a marked improvement in the description of the volumetric properties without losing the descriptive qualities of the liquid–vapor equilibria:

$$P = \frac{RT}{\tilde{V}-\tilde{b}} - \frac{a(T)}{\tilde{V}(\tilde{V}+\gamma\tilde{b})} \quad \text{with} \quad \tilde{V} = V + c \quad \text{and} \quad \tilde{b} = b(2-\sqrt{2}) \tag{6}$$

3.2. SBR Equation of State

Simonet–Behar–Rauzy's [13] equation, which is noncubic, with four parameters, and which differs from SRK's equation through the presence of a multiplying factor for the attraction term, representing a second-degree $1/V$ development:

$$P = \frac{RT}{V-b} - \frac{a}{V(V+b)}\left[1 - \gamma\frac{b}{V} + \delta\frac{b^2}{V^2}\right] \tag{7}$$

3.3. COR Equation of State

The "chain of rotators" equation proposed by Chien–Greenkorn–Chao [14], which can be represented according to the following formulation:

$$\frac{PV}{RT} = 1 + \frac{4\left(\frac{\tilde{V}}{\tau}\right)^2 - 2\left(\frac{\tilde{V}}{\tau}\right)}{\left(\frac{\tilde{V}}{\tau}-1\right)^3} + \frac{c}{2}(\alpha-1)\frac{3\left(\frac{\tilde{V}}{\tau}\right)^2 + 3\alpha\left(\frac{\tilde{V}}{\tau}\right) - (\alpha+1)}{\left(\frac{\tilde{V}}{\tau}-1\right)^3}$$
$$+\left[1 + \frac{c}{2}\left(B_0 + \frac{B_1}{\tilde{T}} + B_2\tilde{T}\right)\right]\sum_{n,m}\frac{m}{\tilde{T}^n}\frac{A_{nm}}{\tilde{V}^m} \tag{8}$$

in which A_{nm}, B_0, B_1, B_2, c, τ, and α are parameter terms and $\tilde{V}$, $\tilde{T}$ are reduced terms.

3.4. LK Correlation

The Lee–Kesler [1] model is an application of the principle of corresponding states involving three parameters (T_r, P_r, ω), which expresses the compressibility factor Z of a system as a function of the system's acentric factor and the compressibility factors $Z^{(0)}$ and $Z^{(r)}$ of two reference substances (respectively assimilated to methane and octane), and which is written

$$Z = Z^{(0)} + \frac{\omega}{\omega^{(r)}} [Z^{(r)} - Z^{(0)}] \tag{9}$$

The quantities $Z^{(0)}$ and $Z^{(r)}$ must be evaluated beforehand by means of a modified 12-parameter Benedict–Webb–Rubin (BWR) [5] equation of state. Two series of 12 numerical values were defined for the various constants, one enabling the evaluation of $Z^{(0)}$ (the simple substance selected by Lee and Kesler being methane), the other that of $Z^{(r)}$ (the superscript "r" being associated with octane, which these authors adopted as a second reference). The verifications were carried out first of all with all the parameters generated by Lee–Kesler (method LK1) and then with a new set of constants recalculated by Muñoz and Reich [6] so as to be able to improve prediction in the liquid phase (method LK2).

To apply an equation of state to a mixture, one should also adopt mixing rules linking the parameters of the mixture to those of the components and their respective proportions. As the Lee–Kesler correlation contains 24 parameters, it does not lend itself to the use of mixing rules on so many parameters; the widely used rules consist in defining, for multicomponent systems, pseudocritical coordinates as a function of those of the components. Different rules of this type have been proposed by

Table V. Absolute Average Deviations (AAD; %) Between Experimental and Ultrasonic Speeds Calculated by Lee–Kesler Using Various Mixing Rules

Mixing rule	Mixture G1	Mixture G2
Lee–Kesler [1]	1.3	0.7
Hankinson–Thomson [17]	1.2	0.7
Pedersen et al. [18]	1.3	0.8
Plocker et al. [19]	1.2	0.7
Teja [20]	1.1	0.7
Spencer–Danner [21]	3.0	2.0

Lee–Kesler [1], Hankinson–Thomson [7], Pedersen et al. [18], Plocker–Knapp–Prausnitz [19], Teja [20], and Spencer–Danner [21]. In the case of this kind of gaseous mixtures, Table V shows that the effect of the choice of the mixing rule makes practically no difference, the best calculation being those provided by the rules proposed by Teja [20]:

$$T_{c_m} V_{c_m} = \sum_{i=1}^{N} \sum_{j=1}^{N} x_i x_j T_{c_{ij}} V_{c_{ij}} \tag{10}$$

$$V_{c_m} = \sum_{i=1}^{N} \sum_{j=1}^{N} x_i x_j V_{c_{ij}} \tag{11}$$

with the crossed parameters $V_{c_{ij}}$ and $T_{c_{ij}}$ obeying

$$V_{c_{ij}} T_{c_{ij}} = (T_{c_i} V_{c_i} T_{c_j} V_{c_j})^{1/2} \tag{12}$$

$$V_{c_{ij}} = (V_{c_i}^{1/3} + V_{c_j}^{1/3})^3/8 \tag{13}$$

and the pseudocritical pressure P_{c_m} of the mixture being obtained by the linear rule of composition on the compressibility factor, while the acentric factor of the mixture results from a direct linear combination.

3.5. AGA8 Model

Corresponding to a modification of the BWR equation, AGA 8 requires several parameters which have been especially tuned to reproduce very accurately the PVT properties of natural gases:

$$Z = 1 + BV^{-1} + CV^{-2} + DV^{-3} + EV^{-5} + A_1 V^{-2}(1 + A_2 V^{-2}) \exp(-A_2 V^{-2}) \tag{14}$$

where A_1, A_2, B, C, D, and E are parameter terms which are functions of temperature and composition. For example, the absolute average deviation of Z is about 0.1% when the pressure ranges from 0.1 to 10 MPa. Associated with the Savidge and Shen [3] procedure, this equation leads to excellent results for the speed of sound up to moderate pressures. This remark matches with the works of Younglove and Frederick [7] on gaseous systems with compositions close to the two examples studied in this paper.

To appreciate the respective abilities of these models, we indicate in Table VI the deviations obtained for the two gases. These deviations, expressed as %, characterize the absolute average deviations (AAD) defined by

$$\delta_r U\,\% = \frac{100}{N} \sum_{i=1}^{N} \left| \frac{U_{i\,\mathrm{cal}} - U_{i\,\mathrm{exp}}}{U_{i\,\mathrm{exp}}} \right| \tag{15}$$

Table VI. AAD (%) Between Experimental and Ultrasonic Speeds Calculated by Various Models

Equation of state	Mixture G1	Mixture G2
SRK	19.3	17.6
PR	9.4	9.7
PR-RP	4.7	3.7
COR	7.8	9.2
SBR	1.7	2.0
LK1	1.1	0.7
LK2	1.0	0.65
AGA 8	0.7	0.6

Study of the prediction results shows the poor representation of the ultrasonic speed by the cubic equations SRK (Fig. 6) and PR (with mean deviations of 18% for SRK and 9% for PR). If the volumetric translation proposed by Rauzy–Peneloux is performed, it is well-known that the prediction of volumetric properties is substantially improved. The same is true of ultrasonic speed, as can be observed from Table VI. This shows that this simple equation of state developed primarily to predict liquid–vapor equilibria, can be improved to predict gaseous properties.

One other equation of state of the six equations used yielded very satisfactory results on gaseous mixtures. This is the SBR equation, which,

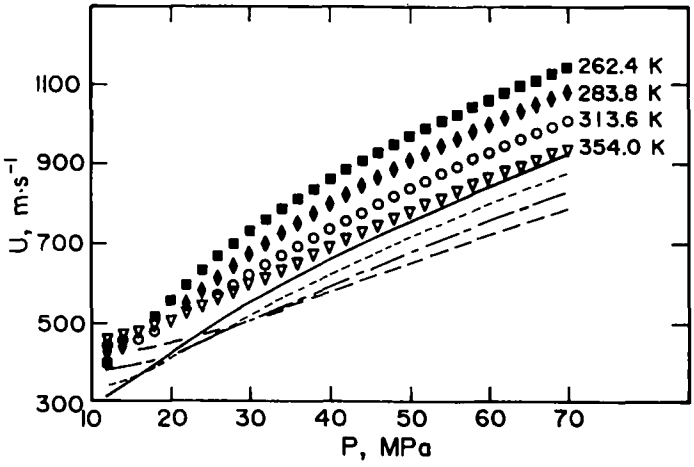

Fig. 6. Comparison of the experimental and calculated ultrasonic speed in sample G1. (——) 262.4 K; (---) 283.8 K; (—·—) 313.6 K; (– – –) 354.0 K. Values calculated with SRK equation of state.

combined with the rule proposed by Jullian [22], gives a mean deviation for the entire range of data of the order of 2%. With this model, the predictions are increasingly accurate with increasing temperature.

Finally these tests reveal a marked deterioration in the predictive abilities of the "chain of rotators" equation in the case of systems in the gaseous state, compared with the very satisfactory results it yields for the liquid state. It should be recalled that in the case of binary or ternary systems containing alkanes, CO_2, and aromatic hydrocarbons studied in single-phase liquid conditions of state, this equation of state generates ultrasonic speed data with a mean deviation of 4–5% from the experimental data, over a wide range of composition, pressure and temperature. The results obtained on the gaseous systems subjected to the above analysis fall a long way short of this performance.

In the case of the Lee–Kesler model, which also performed in a very satisfactory manner when applied to a large number of hydrocarbons in the liquid state, the situation is much better. For the gaseous mixtures considered, real progress can be observed in the quality of predictions, a feature which is no doubt connected with the fact that methane is one of the reference elements in this procedure, based on the principle of corresponding states. In order to demonstrate the quality of data predictions by the Lee–Kesler thermodynamic model, we plotted in Figs. 7 and 8 a few isotherms of the mixtures G1 and G2 deduced from the calculations as well as the experimental points for the same temperatures. It can be verified that the curves generated fit well with the experimental data, at least at pressures

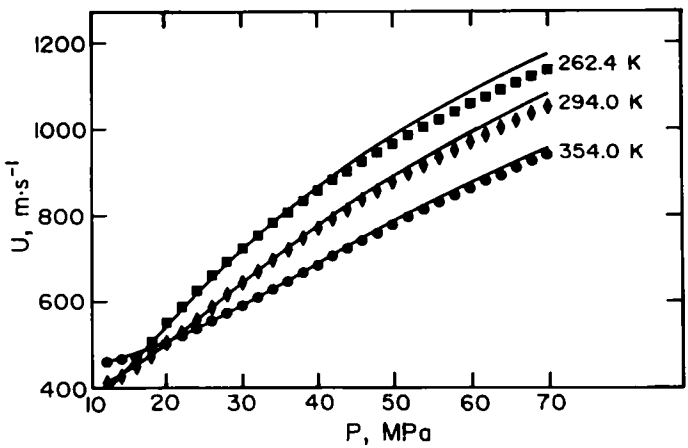

Fig. 7. Comparison of the experimental and calculated ultrasonic speed in sample G1. (——) Values calculated with Lee–Kesler.

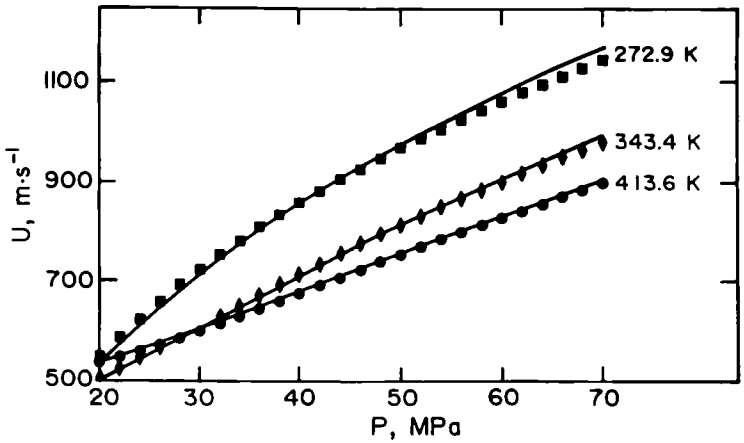

Fig. 8. Comparison of the experimental and calculated ultrasonic speed in sample G2. (——) Values calculated with Lee-Kesler.

up to 50 MPa. In particular, the intersections of the various isotherms and their respective inflections are well reproduced by the model. If the experimental verification base is limited to points associated with pressures lower than or equal to 50 MPa (i.e., 160 points for the system G1 and 176 points for G2), the mean deviations are significantly reduced, 0.53% for G1 and 0.44% for G2, respectively. This performance is all the more remarkable, as the Lee-Kesler model is used in its original form, in other words, without adjustment of the parameters on the ultrasonic speed data.

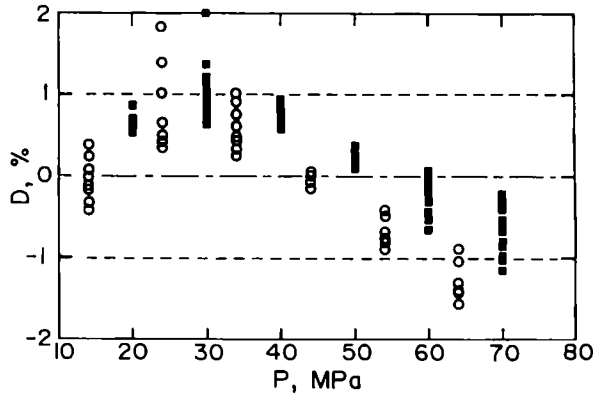

Fig. 9. Deviation (%) between experimental and calculated with AGA 8 ultrasonic speed. (○) Mixture G1; (■) mixture G2.

It is therefore a general all-purpose procedure which was not initially designed to characterize a derived quantity such as that considered here. In the case of mixtures of hydrocarbon components in the liquid state, this method had already proved effective. In the case of systems in the gaseous state, such as those examined in the course of this study, the results that it generates were found to be even more convincing. Even if slight improvement is observed, the LK2 version with the Munoz and Reich [16] parameters does not really modify the results described above. We have also to point out that the AGA 8 equation, originally built in order to characterize the thermodynamic properties of gases up to pressures around 20 MPa, is able to predict consistent values on the whole data base up to 70 MPa within an accuracy about 0.6%. Figure 9 shows the scattering of errors against pressure and we can notice that the maximum deviation error is only 2%.

4. CONCLUSION

One of the problems involved in the production of petroleum fluids is that of the selection of general modeling procedures which can be applied to both the liquid and the gaseous states. In the case of hyperbaric fluids, thermodynamic models, usually applied to fluids whose natural conditions of existence correspond to much lower pressures, frequently prove inadequate. In order to remedy this unsatisfactory situation, it will be necessary either to revise the parameters involved in the classical models or to define new models specifically adapted to these particular fluids. In either of these cases, the operations will be feasible only once a sufficient volume of experimental data on various thermodynamic properties, including ultrasonic speed, has been accumulated. The experimental data reported in this paper are presented in order to contribute to the realisation of this objective, since, at the highest pressures used in the study, the mixtures tested can simulate such fluids.

The numerical verifications, performed on data based on Lee–Kesler's model of corresponding states, demonstrate that this all-purpose procedure has interesting potential as regards the prediction of the behavior of ultrasonic speed in materials in the gaseous state. The SBRJ equation of state also possesses, though to a lesser extent, this ability. However, even in gases (and *a fortiori* in liquids), if the required degree of accuracy is to be very high (less than a few meters per second), a specific procedure for the characterization of ultrasonic speed in the high-pressure domain will be necessary. The very good results of the AGA 8 model above 20 MPa may encourage us to focus our future work on a correction at high pressure of the equation, in order to enhance the predictive potential of the model.

ACKNOWLEDGMENTS

The authors wish to thank D. Ingrain for his hightly appreciated assistance. They are also indebted to the Société GAZ DE FRANCE for technical support.

REFERENCES

1. B. I. Lee and M. G. Kesler, *AIChE J.* **21**:510 (1975).
2. K. E. Starling, *American Gas Association Transmission Measurement Committee Report No. 8* (1985).
3. J. L. Savidge and J. J. S. Shen, *Int. Gas RES. Conf.*, Tokyo, Japan Nov. (1989), pp. 6–9.
4. S. Ye, J. Alliez, B. Lagourette, H. Saint-Guirons, J. Arman, and P. Xans, *Rev. Phys. Appl.* **25**:555 (1990).
5. J. L. Daridon, *Acoustica* **80**:416 (1994).
6. W. Van Dael and A. Van Itterbeek, (North-Holland, Amsterdam, 1965), p. 311.
7. B. A. Younglove and N. V. Frederick, *Int. J. Thermophys.* **11**:897 (1990).
8. S. Ye, B. Lagourette, J. Alliez, H. Saint-Guirons, P. Xans, and F. Montel, *Fluid Phase Equil.* **74**:157 (1992).
9. S. Ye, B. Lagourette, J. Alliez, H. Saint-Guirons, P. Xans, and F. Montel, *Fluid Phase Equil.* **74**:177 (1992).
10. G. Soave, *Chem. Eng. Sci.* **27**:1197 (1972).
11. D. Y. Peng and D. B. Robinson, *Ind. Eng. Chem. Fund.* **15**:59 (1976).
12. A. Peneloux, E. Rauzy, and R. Freze, *Fluid Phase Equil.* **8**:7 (1982).
13. E. Behar, R. Simonet, and E. Rauzy, *Fluid Phase Equil.* **21**:237 (1985).
14. C. H. Chien, R. A. Greenkorn, and K. C. Chao, *AIChE J.* **29**:560 (1983).
15. M. Benedict, G. B. Webb, and L. C. Rubin, *J. Chem. Phys.* **8**:334 (1940).
16. F. Munoz and R. Reich, *Fluid Phase Equil.* **13**:171 (1983).
17. R. W. Hankinson and G. N. Thomson, *AIChE J.* **25**:653 (1979).
18. K. S. Pedersen, A. Fredenslund, P. L. Christensen, and P. Thomassen, *Chem. Eng. Sci.* **39**:1011 (1984).
19. U. Plocker, H. Knapp, and J. Prausnitz, *Ind. Eng. Chem. Process Des. Dev.* **17**:324 (1978).
20. A. S. Teja, *AIChE J.* **26**:337 (1980).
21. C. F. Spencer and R. P. Danner, *J. Chem. Eng. Data* **17**:236 (1972).
22. S. Jullian, Thèse de Doctorat (ENSPM, Paris, France, 1988).